Received: 2 June 2021 | Revised: 21 July 2021 | Accepted: 30 July 2021

DOI: 10.1002/jcla.23961

RESEARCH ARTICLE

WILEY

Distinguishing colorectal adenoma from hyperplastic polyp by WNT2 expression

Bangting Wang[1] | **Xin Wang**[2] | **Yujen Tseng**[1] | **Meina Huang**[2] | **Feifei Luo**[1] | **Jun Zhang**[1] | **Jie Liu**[1]

[1]Department of Digestive Diseases, Huashan Hospital, Fudan University, Shanghai, China

[2]State Key Laboratory of Genetic Engineering, School of Life Sciences, Fudan University, Shanghai, China

Correspondence
Jie Liu, Department of Digestive Diseases, Huashan Hospital, Fudan University, Shanghai 200040, China.
Email: jieliu@fudan.edu.cn

Funding information
This work was supported by the National Key Science and Technology Project of China (2018YFC2000500-03), the National Natural Science Foundation of China (81630016), and the Shanghai Municipal Key Clinical Specialty (shslczdzk05903).

Abstract

Background: Colorectal adenoma (CRA) is a classical premalignant lesion, with high incidence and mainly coexisting with hyperplastic polyp (HPP). Hence, this study aimed to distinguish CRA from HPP by molecular expression profiling and advance the prevention of CRA and its malignance.

Methods: CRA and paired HPP biopsies were collected by endoscopy. Through RNA-sequencing (RNA-seq), the differentially expressed genes (DEGs) were obtained. Functional enrichment analysis was performed based on the DEGs. The STRING database and Cytoscape were used to construct the protein-protein interaction (PPI) network and perform module analysis. Hub genes were validated by real-time quantitative PCR (RT-qPCR) and immunohistochemistry. The ROC curve was drawn to establish the specificity of the hub genes.

Results: 485 significant DEGs were identified including 133 up-regulated and 352 down-regulated. The top 10 up-regulated genes were *DLX5*, *MMP10*, *TAC1*, *ACAN*, *TAS2R38*, *WNT2*, *PHYHIPL*, *DKK4*, *DUSP27*, and *ABCA12*. The top 10 down-regulated genes were *SFRP2*, *CHRDL1*, *KBTBD12*, *RERGL*, *DPP10*, *CLCA4*, *GREM2*, *TMIGD1*, *FEV*, and *OTOP3*. Wnt signaling pathway and extracellular matrix (ECM) were up-regulated in CRA. Three hub genes including *WNT2*, *WNT5A*, and *SFRP1* were filtered out via Cytoscape. Further RT-qPCR and immunohistochemistry confirmed that WNT2 was highly expressed in CRA. The area under the ROC curve (AUC) at 0.98 indicated the expression level of WNT2 as a candidate to differ CRA from HPP.

Conclusion: Our study suggests Wnt signaling pathway and ECM are enriched in CRA, and WNT2 may be used as a novel biomarker for distinguishing CRA from HPP and preventing the malignance of CRA.

KEYWORDS
bioinformatics, colorectal adenoma, extracellular matrix, hyperplastic polyp, Wnt signaling pathway, WNT2

1 | INTRODUCTION

Colorectal adenoma (CRA) is a benign tumor originating from the glandular epithelium of the colorectal mucosa. Its pathological classification includes tubular adenoma, villous adenoma, and villous tubular adenoma. About 85% of colorectal cancers (CRCs) are sporadic and progress slowly by accumulating multiple genetic mutations (APC, KRAS, p53, and SMAD4) in precancerous lesions (CRA).[1] This process is referred to as adenoma-carcinoma sequence, which usually takes 5–15 years.[2] Presently, adenomas are divided into two categories, namely low-risk adenoma and high-risk adenoma. High-risk adenomas are larger than 10 mm in diameter, villous or tubulovillous adenoma, and/or exhibit high-grade dysplasia, which are considered to be clinical precursors of CRC. The incidence of CRA is gradually increasing for different risk factors, such as genetic background, diet, smoking, alcohol, and exercise.[3] Most CRAs are found in the distal part of the colon, which includes the sigmoid colon and rectum.[4]

Hyperplastic polyp (HPP) is benign, non-cancerous lesions, usually with a maximum size of 1–5 mm. Recent studies have shown that hyperplastic polyps often coexisted with adenoma and adenocarcinoma and had biological commonalities with colorectal cancer, such as secretion of peptides and mucin.[5,6] So, we need to pay attention to HPP for the same characteristics with CRC even though its malignant potential is low.

Currently, the pathologic diagnosis of HPP and CRA mainly relies on histopathological examination to observe epithelial morphological changes, lacking specific diagnostic markers. Some researches have reported the microRNA profiles and gene signature between HPPs, serrated polyps/adenomas, and CRCs.[7,8] However, the difference in gene expression profiles between HPP and CRA is still unclear and has not been elaborated in detail. Studying the natural history of HPP and CRA, including how HPP evolves into CRA, is challenging because once HPP and CRA are found during the examination, they will be removed endoscopically. So, the gene expression differences between HPP and CRA, and which signaling pathways and genes play vital roles in the transition from HPP to CRA or progression of CRA are not yet known.

RNA-sequencing is used to analyze differentially expressed genes (DEGs) at the whole transcriptome level to determine the specific expression profiles of the studied samples. Based on RNA-sequencing results, bioinformatics can conduct functional enrichment analysis and select hub genes from DEGs to distinguish different clinical samples, such as tumor and adjacent normal tissue. So, it is of great significance to study the differential expression profiles of HPP and CRA and explore colon tumor progression in depth using bioinformatics.

We hypothesized that RNA-sequencing can effectively obtain the differential expression profile of HPP and CRA, and bioinformatic analysis further can find specific biomarkers. In this study, we aimed to detect the differences in transcriptome between HPP and CRA by RNA-sequencing and identify differential functional pathways or hub genes between CRA and HPP, which may shed light on the pathogenesis and evolution of HPP and CRA.

2 | MATERIALS AND METHODS

2.1 | Tissues

Fresh CRA and paired HPP biopsies were collected from the Endoscopy Center of Huashan Hospital, Fudan University, after pathologic identification by two independent pathologists (Table 1). Histopathological sections CRA and HPP were obtained from the Department of Pathology, Huashan Hospital, Fudan University (Table S1).

This research was conducted according to the Declaration of Helsinki and was approved by the Ethical Committee of Huashan Hospital, Fudan University (2018–182). Informed consent had been obtained from all subjects involved and the project.

2.2 | RNA-sequencing (RNA-seq)

RNA was extracted using RNeasy Mini Kit (Qiagen) following manufacturer's instructions and then converted into cDNA library by GoscriptTM reverse transcription system (Promega) for high-throughput sequencing. More than 45 million reads were received per sample from HiSeq platform for 4 biological replicates. The

TABLE 1 Clinical information of biopsy samples for RNA-seq

	Sex	Age	Size (mm)	Location	Pathology
P1	Female	53	6 × 6	Descending colon	Hyperplastic polyp
			10 × 15	Sigmoid colon	Tubular adenoma
P2	Man	65	5 × 5	Descending colon	Hyperplastic polyp
			25 × 30	Descending colon	Tubular adenoma
P3	Man	65	4 × 5	Descending colon	Hyperplastic polyp
			12 × 15	Descending colon	Tubular adenoma with intraepithelial neoplasia
P4	Man	68	3 × 4	Sigmoid colon	Hyperplastic polyp
			8 × 10	Sigmoid colon	Tubular adenoma

Abbreviation: P, patient.

RNA-seq data were uniquely mapped to the Hg19 genome by HISAT (V0.1.6-beta) and only the uniquely mapped reads were used to estimate the expression values in gene level by RPKM. Expression values were assigned to gene level by RSEM (v1.2.12).[9]

2.3 | Identification of DEGs among RNA-seq data

To investigate DEGs among HPP and CRA, the limma package in R was used with the cutoff criteria of |log 2-fold-change [FC]| >1 and *p*-value <0.05. The differential genes co-expressed by functional pathway analysis and MCODE module 1 were obtained from http://bioinformatics.psb.ugent.be/webtools/Venn/.

2.4 | GO (Gene Ontology) and KEGG (Kyoto Encyclopedia of Genes and Genomes) pathway enrichment analysis

To explore the biological functional roles of DEGs, the Database for Annotation, Visualization, and Integrated Discovery (DAVID, https://david.ncifcrf.gov/) was used to perform functional enrichment analysis to identify GO categories. With reference from KEGG pathways, the DAVID database was also applied for pathway enrichment analysis. *p*-value <0.05 was considered statistically significant.

2.5 | Gene set enrichment analysis

DEGs between hyperplastic polyp and adenoma were analyzed by gene enrichment analysis to characterize adenoma by comparing the obtained gene sets to known disease-related gene sets. Gene set enrichment analysis (GSEA; http://software.broadinstitute.org/gsea/) was employed to classify and highlight functionally distinct biologic features of the colorectal adenomas.

2.6 | Establishment of PPI network

To construct the PPI network, the STRING (version 11.0; http://string-db.org/; Szklarczyk et al., 2020) online database was used. Cytoscape (version 3.8.2) software (http://www.cytoscape.org/) was used to visualize and analyze the PPI network. The MCODE plug-in of the Cytoscape software was used to screen important modules of the entire network.

2.7 | RT-qPCR and immunohistochemistry

Total RNA of HPPs and CRAs was extracted utilizing the RNeasy Protect Mini Kit (Qiagen). The GoscriptTM reverse transcription system (Promega) was used to reverse transcription of RNA. Each PCR was carried out in a 15 μL volume using SYBR Green Master mix (Vazyme) for 15 min at 95°C for initial denaturing, followed by 40 cycles of 95°C for 30 s and 60°C for 1 min in the 7500 fast real-time PCR system (Applied Biosystems). Primers used were listed in Table S2.

5 μm adenoma and hyperplastic polyp sections were prepared for hematoxylin-eosin staining for morphological analysis. Sections were orderly deparaffinized in a series of xylene baths, then rehydrated using a graded alcohol series, and retrieved in sodium citrate buffer (pH 6.0) via pressure cooker heating for 15 min. The WNT2 antibody was used for IHC at a 1:300 dilution incubated at 4°C overnight. Secondary antibody was incubated at room temperature for 60 min, and the horseradish peroxidase solution was incubated for 30 min and performed with diaminobenzidine (DAB) according to manufacturer's recommendations (GBI, USA) and subsequently counterstained with hematoxylin. The IHC staining scores were classified into four score ranks: 0, negative; 1, weak; 2, moderate; and 3, strong.[10]

2.8 | ROC and AUC

SPSS software was used for ROC analysis of WNT2 (version 20.0, SPSS Inc). ROC and AUC were utilized to evaluate the predictive value of WNT2 for CRA.

2.9 | Statistical analysis

We employed Student's *t* test to analyze the experimental results. Data analysis was performed by GraphPad Prism 7 statistical software. Statistical significance was considered at $p < 0.05$.

3 | RESULTS

3.1 | DEGs between CRA and HPP

Four CRA and paired HPP with histologic diagnosis were enrolled for gene expression profiles analysis (Figure 1A). By integrated bioinformatics analysis between CRA and HPP (Figure 1B), 485 DEGs were identified, including 133 up-regulated genes and 352 down-regulated genes in CRA, compared with HPP. The volcano plot and heatmap of DEGs were constructed (Figure 1C, 1D), indicating the variance of molecular expression profiles between CRA and HPP. The top 10 up- and down-regulated genes were listed in Table 2.

3.2 | Wnt signaling pathway, stem-related genes, and extracellular matrix genes are significantly enriched in CRA

To gain insight into the molecular function of DEGs, GO and KEGG pathway enrichment analysis were implemented. In GO analysis, the main terms included proteinaceous

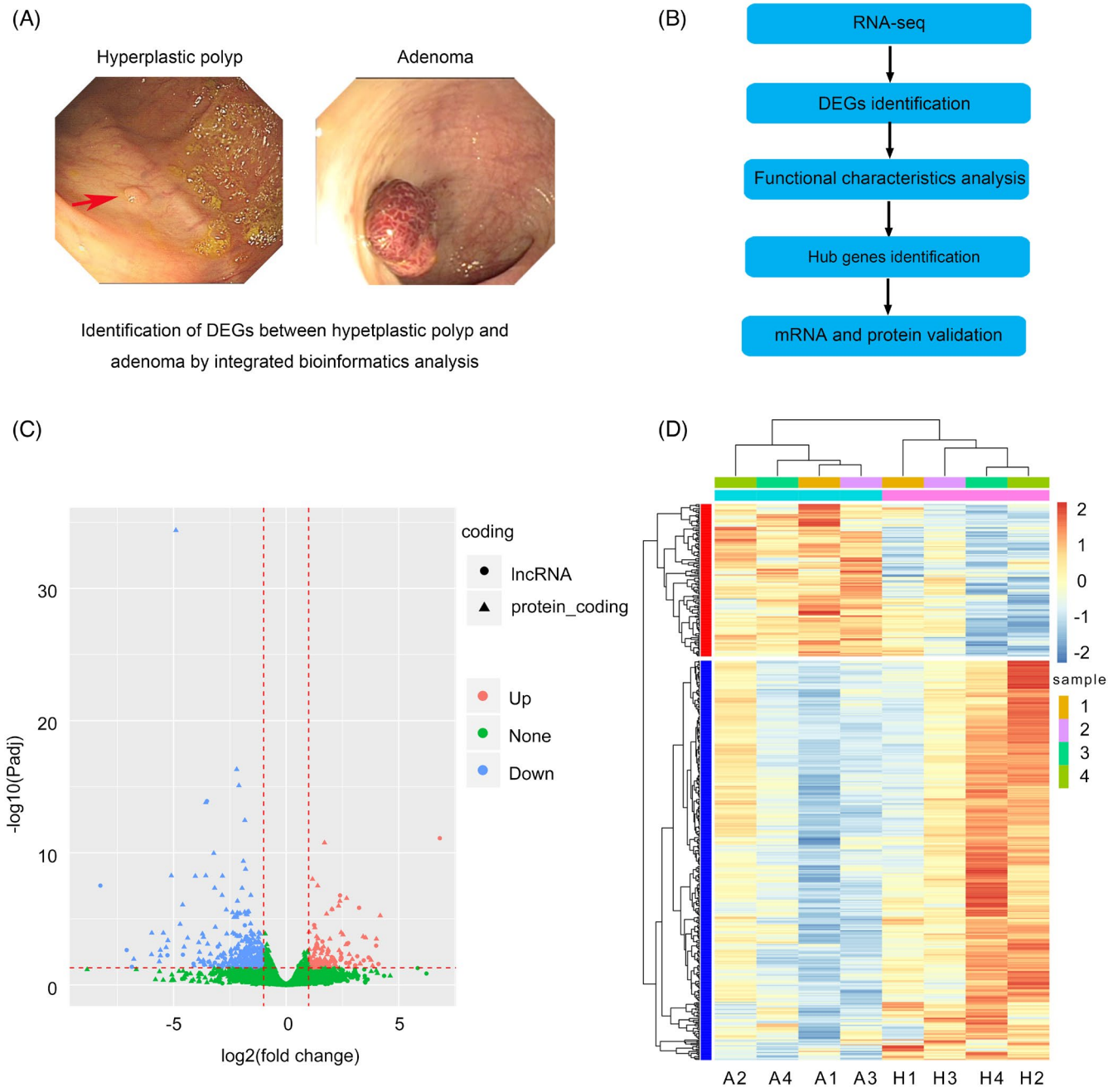

FIGURE 1 Identification DEGs between HPP and CRA *via* bioinformatics. (A). Bright-field images of hyperplastic polyp and adenoma taken by endoscopy in the colon. (B). Flow diagram of the present study. (C). Volcano plots of the distribution of DEGs in RNA-seq. (D). Expression heatmap of the robust DEGs (133 up-regulated genes; 352 down-regulated genes). |Fold change| >1. A, colorectal adenoma; DEGs, differentially expressed genes; H, hyperplastic polyp

extracellular matrix (p = 1.91384E-12), serine−type endopeptidase activity (p = 4.54499E-09), and immune response (p = 1.17644E-06) (Figure 2A). In addition, KEGG analysis indicated that Wnt signaling pathway (p = 0.0004), Chemokine signaling pathway (p = 0.0101), and cytokine-cytokine receptor interaction (p = 0.0212) were the significantly enriched pathways (Figure 2B). Subsequently, GSEA was performed to predict the biological function of DEGs. The results showed that *NANOG*, *SOX2*, and extracellular matrix were significantly enriched in CRA (Figure 3A-C).

3.3 | Significant hub genes are selected by PPI network construction and MCODE

To further explore the biological roles of these DEGs, the STRING database was used to create a PPI network based on significant difference genes (Top 50) (Figure 4A). In this network, there were 19 up-regulated and 31 down-regulated genes. Then, using MCODE, the top 1 module was identified from the whole network (Figure 4B), which was made up of 11 nodes and 26 edges. Significant hub genes

TABLE 2 The list of top 20 up-regulated and down-regulated differentially expressed genes

Rank	Symbol	Average of HPP	Average of CRA	Log2FoldChange	*p*-value	Significance
1	DLX5	3.501009477	4.756421158	4.180038889	1.20E−08	UP
2	MMP10	5.051111908	6.509282601	4.009207984	1.29E−06	UP
3	TAC1	3.066136511	3.996374331	3.841876875	0.00087753	UP
4	ACAN	3.406017057	4.358215265	3.770304802	0.00017328	UP
5	TAS2R38	3.642724232	4.620123178	3.53158358	9.75E−07	UP
6	WNT2	4.527152153	5.831657474	3.42505357	7.76E−07	UP
7	PHYHIPL	3.686947777	4.539733517	3.296953498	0.00053998	UP
8	DKK4	3.242646697	3.957578361	3.284117569	0.00050348	UP
9	DUSP27	4.367751787	5.85584151	3.05784227	0.00115139	UP
10	ABCA12	4.838709294	6.343218871	2.938013634	0.00014315	UP
11	SFRP2	6.592489901	4.764402889	−6.765548095	0.00013468	DOWN
12	CHRDL1	6.678674414	4.758218521	−5.979011071	4.58E−05	DOWN
13	KBTBD12	8.923494797	6.542188724	−5.967411777	3.21E−07	DOWN
14	RERGL	3.976659705	3.167491788	−5.634827035	0.00026457	DOWN
15	DPP10	7.118850115	5.163112407	−5.587270037	1.65E−05	DOWN
16	CLCA4	13.46809858	11.44562085	−5.584244147	6.06E−05	DOWN
17	GREM2	7.919251962	5.65555548	−5.454708921	3.29E−07	DOWN
18	TMIGD1	9.967178495	7.708848642	−5.330780732	8.39E−06	DOWN
19	FEV	5.27739316	4.02263553	−5.251395778	1.83E−06	DOWN
20	OTOP3	4.607076228	3.196882483	−5.098981126	3.29E−12	DOWN

Abbreviations: CRA, colorectal adenoma; HPP, hyperplastic polyp.

were selected from the top 1 module including *SAA1*, *CCL19*, *CCXR3*, *NPY*, *WNT2*, *WNT5A*, *SFRP1*, *SFRP2*, *SOX2*, *AXIN2*, and *PTGER3*.

Through GO and KEGG analysis, we found Wnt signaling pathway ($p = 0.0004$) and proteinaceous extracellular matrix ($p = 1.91 \times 10^{-12}$) contributed to the progression of CRAs (Figure 4C). To identify novel DEGs in adenomas, the two pathways (marked in red in Figure 2 A and B) and MCODE module 1 were overlapped by the Venn diagram. Through screening, we finally identified three genes (*WNT2*, *WNT5A*, and *SFRP1*) that might be specific biomarkers for CRAs (Figure 4D).

3.4 | Both mRNA and protein levels of WNT2 in primary human CRA samples are up-regulated compared with those in HPP samples

The differential genes expression results were verified by RT-qPCR. RT-qPCR of these selected genes (*WNT2*, *WNT5A*, and *SFRP1*) was performed in 10 pairs of HPP and CRA. The results indicated the mRNA level of *WNT2* was similarly up-regulated to the bioinformatic analysis, while the *WNT5A* and *SFRP1* had none significant difference despite the changing trend (Figure 5A-C). We next analyzed the predictive power of WNT2 expression levels for diagnostic purposes by generating ROC curves and c statistic (AUC; Figure 5D). Area under the curve values of 0.98 was observed for WNT2. To further validate difference in WNT2 between HPP and CRA at protein level, we measured its expression in 20 subjects including HPP (n = 9) and CRA (n = 11) by immunohistochemistry. Hematoxylin-eosin staining showed morphological changes from HPP to CRA. In adenomas, the glands were tightly arranged, and the lumen area was reduced (Figure 5E). Notably, robust WNT2 expression was observed in most of adenomas, while its expression in HPP is relatively low. Immunohistochemistry scores for WNT2 expression in HPP and CRA ($p = 0.0147$) were shown in Figure 5F. Altogether, these data indicate that the expression of WNT2 increases from HPP to adenoma.

4 | DISCUSSION

In this study, we focused on the gene expression profiles of sporadic hyperplastic polyps and adenomas through comprehensive bioinformatic analysis and discovered significant enrichment signaling pathways and hub genes. GO and KEGG showed Wnt signaling pathway and extracellular matrix (ECM) were highly expressed in CRA. Besides, GSEA indicated stem-related genes (*NANOG* and *SOX2*) and ECM were highly expressed in CRA. The top regulated genes including *MMP10*, *TAC1*, *ACAN*, *WNT2*, *DKK4*, and *SFRP2* were involved in Wnt signaling pathway and ECM. It has already been shown that these genes play important roles in different cancers. For example, stromal MMP10 drives invasive growth of hypoxic pancreatic ductal adenocarcinoma.[11] SFRP2 modulates

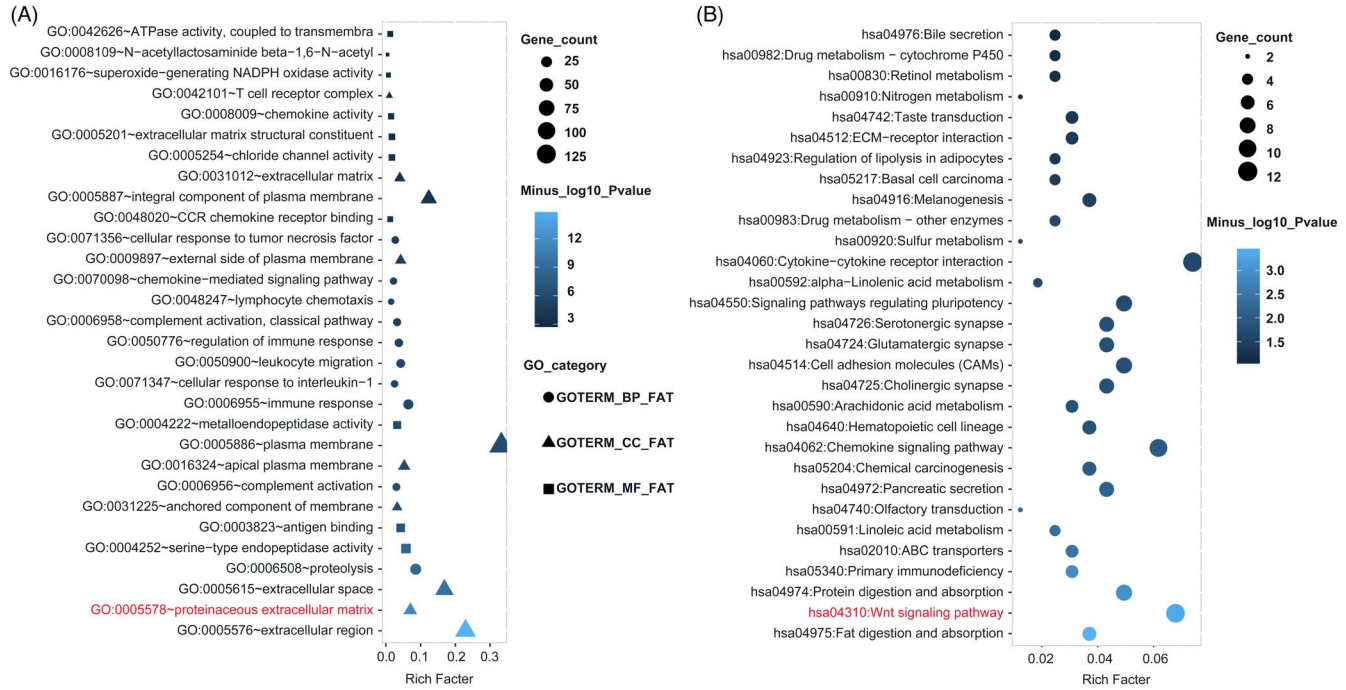

FIGURE 2 Functional enrichment analysis for DEGs from RNA-seq. (A). GO terms (Top 30) found in these DEGs from biological process (BP), cell component (CC), and molecular function (MF). (B). KEGG pathway enrichment analysis of DEGs, and the top 30 were listed. DEGs, differentially expressed genes

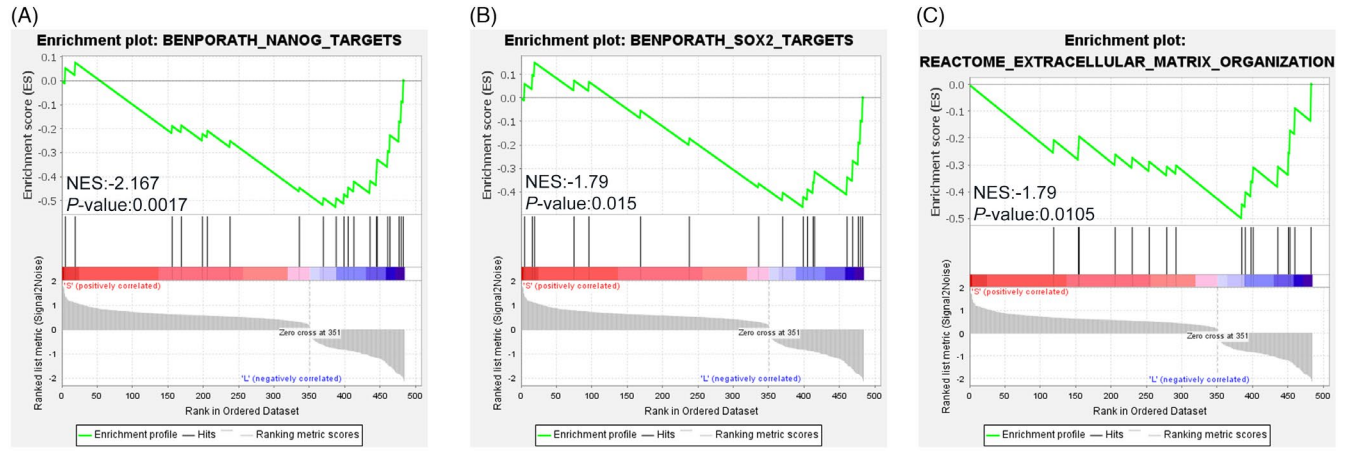

FIGURE 3 Enrichment plots from the GSEA analysis results. (A-C) Several pathways and biological processes were differentially enriched in CRA from HPP, including NANOG targets (p-value =0.0017, NES = −2.167), SOX2 targets (p-value =0.015, NES = −1.79), and extracellular matrix (p-value =0.0105, NES = −1.79). NES, normalized enrichment score

epithelial-mesenchymal transition and stemness via Wnt/β-catenin signaling in choriocarcinoma.[12]

Extracellular matrix (ECM) is a complex extracellular mixture of a variety of biological molecules and fibers secreted by cells in multicellular biological tissues. The intestinal stem cell (ISC) surrounding environment, namely the ISC niche, crucially maintains ISC homeostasis. This niche consists of the supportive mesenchymal cells, fibroblasts as the dominant population, and the differentiated epithelial progeny, all secreted factors including ECM tightly regulating ISC self-renewal, as well as the proliferation and differentiation processes along the crypt.[13] Under pathological contexts, such as chronic inflammation or cancer, ECM biomechanical properties are extremely modified, involving in the development and progression of inflammatory bowel disease and colorectal cancer.[14,15] The tumor microenvironment (TME) mainly includes stem and differentiated cancer cells, and the extracellular matrix.[16] The microenvironment provides a superior condition for the initiation, proliferation, and metastasis of cancers. Cancer stem cells (CSCs) have a strong self-renewal ability and expand through symmetrical split to excessively increase cell growth, ultimately leading to tumor formation.[17] As

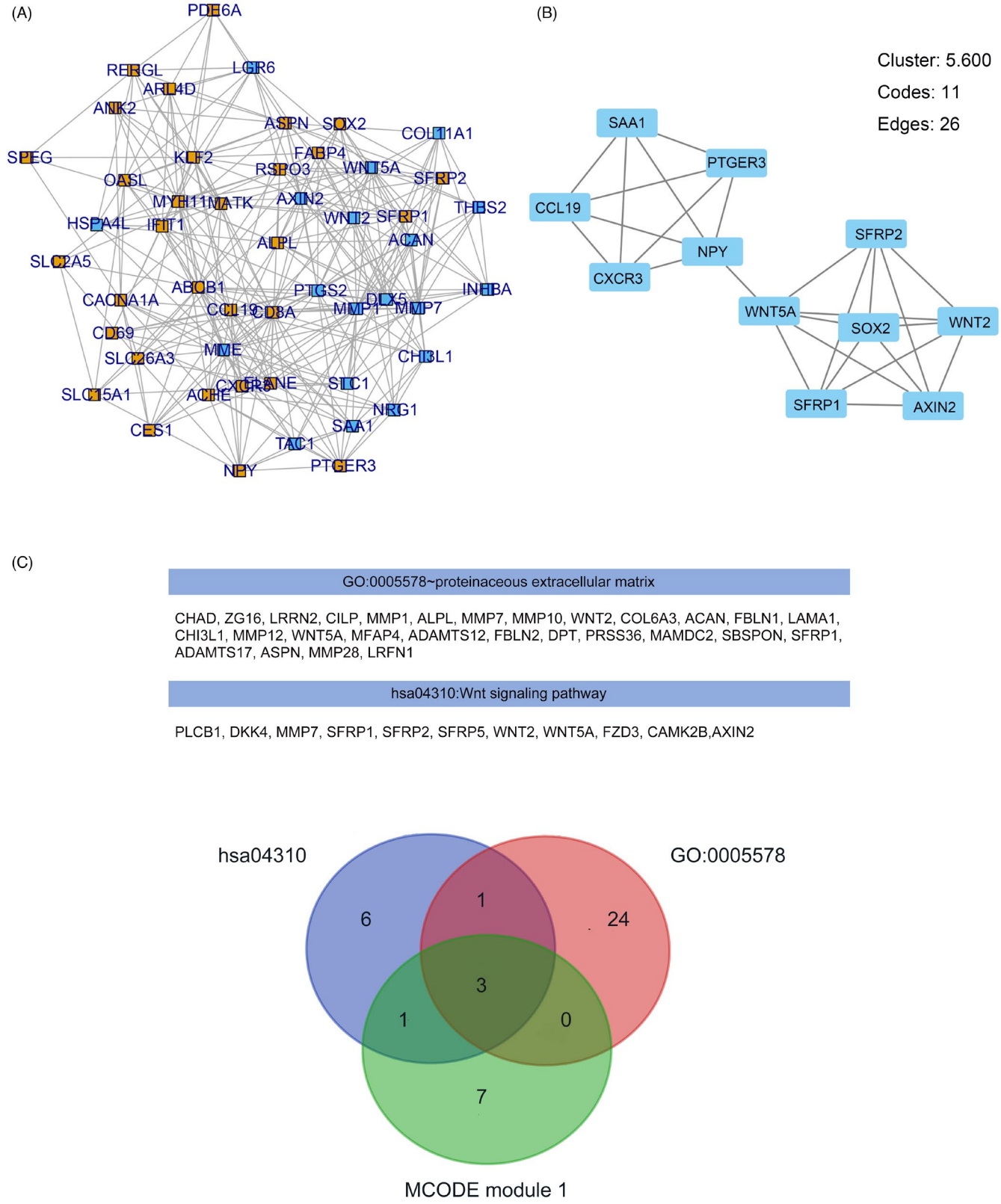

FIGURE 4 Screening the hub genes from module 1 and functional enrichment analysis. (A) Entire PPI network of TOP 50 genes. Blue, up-regulated genes; orange, down-regulated genes. (B) PPI network of top module 1 including 11 nodes and 26 edges. (C). Among the DEGs, genes contained in the Wnt signaling pathway and ECM were listed. (D). Venn diagram of mutual hub genes (*WNT2*, *WNT5A*, and *SFRP1*) based on MCODE module 1 and two functional enrichment pathways. PPI, protein-protein interaction. ECM, extracellular matrix

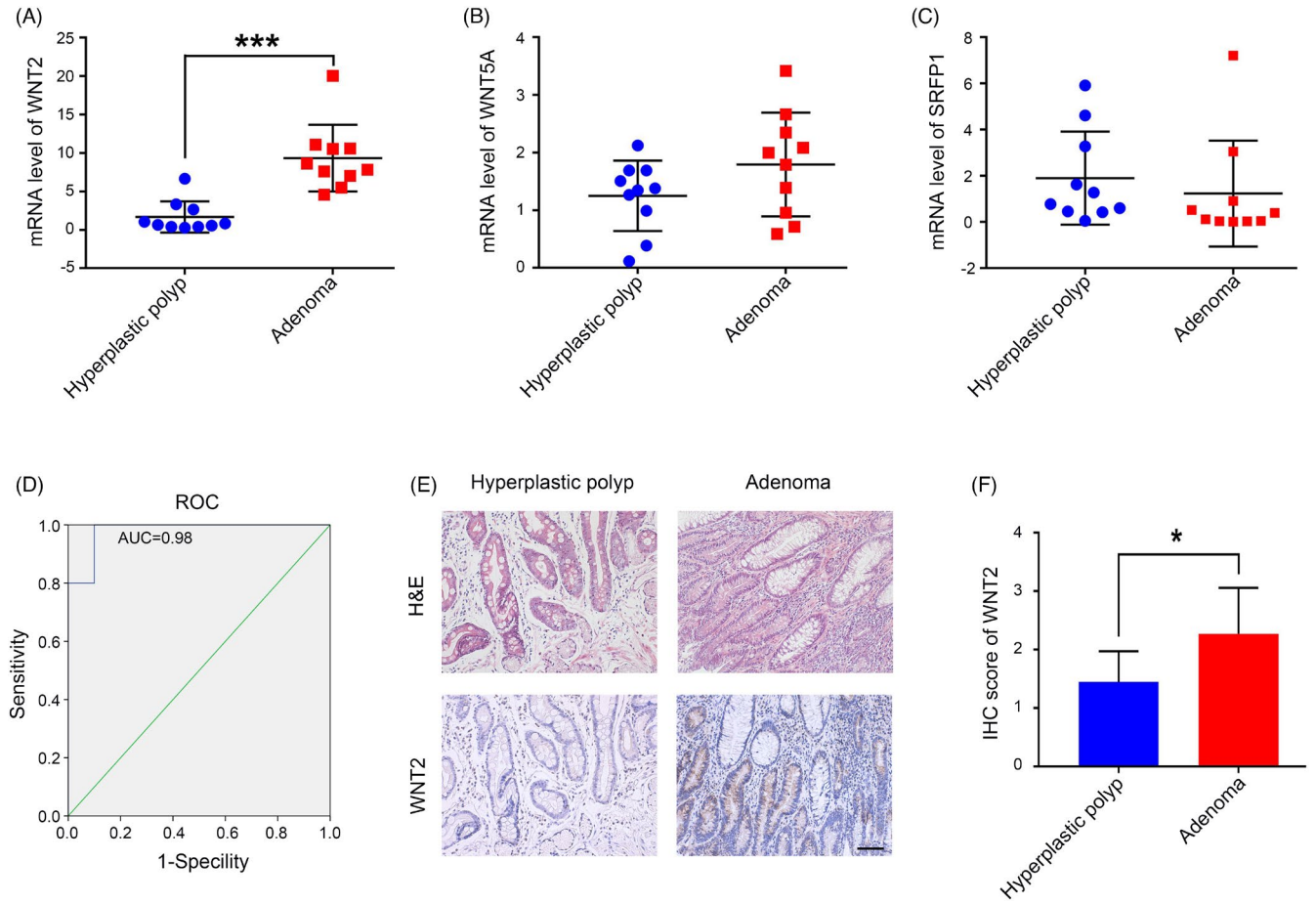

FIGURE 5 RT-qPCR and immunohistochemical staining for the expression of WNT2 in HPP and CRA. (A-C). The relative expression of *WNT2* between hyperplastic polyps and adenoma by RT-qPCR (p-value <0.01). *WNT5A* and *SFRP1* had no significant difference. (D). ROC curves with corresponding AUC values for WNT2 when classifying CRA and HPP. (E). Hematoxylin-eosin staining showed the morphologic structures of hyperplastic polyp and adenoma; Immunohistochemical (IHC) staining showed the expression status of the WNT2. (F). IHC score of WNT2 in hyperplastic polyps and adenoma. (p-value <0.01). *** indicates $p < 0.001$. * indicates $p < 0.05$. NS, no significance; Black scale bar, 200 μm

an integral part of the microenvironmental niche, the ECM components play important roles in anchoring the CSCs to the niche and maintaining stem cell homeostasis.[18] In the TME, ECM has different compositions, organization, and posttranscriptional modification from the surrounding normal tissue and greatly affects the signal transduction, transport mechanism, cell motility, metastasis, and immune response.[19-22] The ECM components such as collagen and hyaluronan form a significant part of the pancreatic tumor.[23] From HPP to CRA, ECM signaling pathway was activated, which could provide unique biochemical, biophysical, and biomechanical properties for CSC niche homeostasis and proliferation of epithelium. Overactive ECM may contribute to the evolution of HPP into CRA and the progression of CRA.

Nanog and SOX2, well-known stem cell markers, contribute to the development of CRC.[24] The inhibition of Nanog and SOX2 can reduce the proliferation of colorectal cancer stem cells.[25,26] Here, we identified Nanog and SOX2 were enriched in adenomas, suggesting that they may contribute to the development and evolution of adenomas.

Wnt signaling pathway can be activated by extracellular secreted proteins (such as some members of the Wnt family). Wnt ligands bind to Frizzled (Fzd) receptors and low-density lipoprotein receptor-related proteins 5 and 6 co-receptors, which lead to the activation of canonical and non-canonical pathways.[27] Wnt signaling is tightly regulated in embryonal development and tissue homeostasis.[28] The gastrointestinal epithelium depends on the accurate regulation of the Wnt signaling pathway to regulate stem cell maintenance, proliferation, and cell lineage differentiation.[29] WNT2 protein has an important role in tumorigenesis of several human cancers including ovarian cancer, esophageal cancer, non-small-cell lung cancer, pancreatic cancer, and gastrointestinal cancer.[30-32] Activation of the Wnt pathway contributes to an increase in proliferation rate, which is sufficient to initiate CRA formation, and mutations in key components of the Wnt pathway are found in more than 90% of colon cancer.[33] In our study, GO analysis revealed that ECM was enriched in CRA. By overlapping MCODE module 1, Wnt signaling pathway, and ECM, we obtained hub genes (*WNT2*, *WNT5A*, and *SFRP1*). Compared with HPPs, WNT2 transcription and protein level were

highly expressed in adenomas confirmed by RT-qPCR and immunohistochemistry. WNT2 can effectively distinguish between HPP and CRA. Meanwhile, as a ligand of the Wnt family, WNT2 can effectively activate the Wnt/beta-catenin signaling pathway. So, WNT2 may promote the proliferation of polyp epithelium and its evolution into adenoma.

Bioinformatics can screen possible biomarkers for tumor and predict its prognosis. It can be used as prediction, with the aim to guide further investigation. It can also be used to analyze the data, provided that the study design is hypothesis-driven. Based on the RNA-seq of HPP and CRA, we screened out the significant gene *WNT2* and enrichment pathways (Wnt signal pathway and ECM) via bioinformatics, which provide a reliable theoretical basis for the functional research of our target genes and enrichment pathways.

Although our research mainly focuses on revealing the different molecular expression profiles between HPP and CRA and screening of significant biomarkers, this will promote our next research progress. We will further study the role of Wnt signaling pathway in the progress of CRA and to characterize the relevance of WNT2 expression to cancer development and its biological functions in the transition from HPP to CRA. For example, whether knockdown of WNT2 in CRA could prohibit adenoma proliferation, and overexpression of WNT2 in HPP promotes its evolution to adenoma. In addition, we will clarify the role of ECM in the progression of adenomas by co-incubating polyp epithelial cells with stromal cells.

5 | CONCLUSION

Collectively, we found that the Wnt-related stem pathway and ECM enriched in CRAs through the bioinformatic analysis of the DEGs between HPP and CRA. Meanwhile, we identified that WNT2 was highly expressed in CRA, which may be as a novel biomarker for CRA. As a ligand of the Wnt pathway, and WNT2 may promote the transformation of HPP to adenoma and contribute to the proliferation of CRA.

ACKNOWLEDGMENTS

We thank Jianping Huang, Weiru Jiang, Wenjie Yue, Jian Chen, and Weiqun Ding for their clinical samples assistance.

CONFLICT OF INTEREST

The authors declare no competing interests.

AUTHOR CONTRIBUTIONS

B.W. designed the experiments. B.W. and X.W. performed the experiments. B.W., J.Z. and M.H. analyzed the data. F.L. and J.L. supervised the work. Y.T., J.Z., B.W., and F.L. wrote the manuscript.

DATA AVAILABILITY STATEMENT

The data that support the findings of this study are available from the corresponding author upon reasonable request.

ORCID

Jie Liu https://orcid.org/0000-0002-7638-187X

REFERENCES

1. Smit W, Spaan C, Johannes de Boer R, et al. Driver mutations of the adenoma-carcinoma sequence govern the intestinal epithelial global translational capacity. *P Natl Acad Sci USA*. 2020;117:25560-25570.
2. Vacante M, Ciuni R, Basile F, Biondi A. Gut microbiota and colorectal cancer development: a closer look to the adenoma-carcinoma sequence. *Biomedicines*. 2020;8(11):489.
3. Castellsagué E, Rivera B, Foulkes W. Colorectal Adenomas. *N Engl J Med*. 2016;375:389.
4. Boroff ES, Gurudu SR, Hentz JG, Leighton JA, Ramirez FC. Polyp and adenoma detection rates in the proximal and distal colon. *Am J Gastroenterol*. 2013;108(6):993-999.
5. Hanby A, Poulsom R, Singh S, et al. Hyperplastic polyps: a cell lineage which both synthesizes and secretes trefoil-peptides and has phenotypic similarity with the ulcer-associated cell lineage. *Am J Pathol*. 1993;142:663-668.
6. Krishn S, Kaur S, Smith L, et al. Mucins and associated glycan signatures in colon adenoma-carcinoma sequence: Prospective pathological implication(s) for early diagnosis of colon cancer. *Cancer Lett*. 2016;374:304-314.
7. Tsikitis V, Potter A, Mori M, et al. MicroRNA Signatures of Colonic Polyps on Screening and Histology. *Cancer Prev Res (Phila)*. 2016;9:942-949.
8. Kanth P, Bronner M, Boucher K, et al. Gene signature in sessile serrated polyps identifies colon cancer subtype. *Cancer Prev Res (Phila)*. 2016;9:456-465.
9. Li BO, Dewey CN. RSEM: accurate transcript quantification from RNA-Seq data with or without a reference genome. *BMC Bioinformatics*. 2011;12(1):323.
10. Liu XF, Li XY, Zheng PS, Yang WT. DAX1 promotes cervical cancer cell growth and tumorigenicity through activation of Wnt/beta-catenin pathway via GSK3beta. *Cell Death Dis*. 2018;9:339.
11. Liu D, Steins A, Klaassen R, et al. Soluble compounds released by hypoxic stroma confer invasive properties to pancreatic ductal adenocarcinoma. *Biomedicines*. 2020;8(11):444.
12. Zeng X, Zhang Y, Xu H, et al. Secreted frizzled related protein 2 modulates epithelial-mesenchymal transition and stemness via Wnt/β-catenin signaling in choriocarcinoma. *Cell Physiol Biochem*. 2018;50:1815-1831.
13. Onfroy-Roy L, Hamel D, Foncy J, Malaquin L, Ferrand A. Extracellular matrix mechanical properties and regulation of the intestinal stem cells: when mechanics control fate. *Cells*. 2020;9(12):2629.
14. Romero-López M, Trinh A, Sobrino A, et al. Recapitulating the human tumor microenvironment: Colon tumor-derived extracellular matrix promotes angiogenesis and tumor cell growth. *Biomaterials*. 2017;116:118-129.
15. de Bruyn M, Vandooren J, Ugarte-Berzal E, et al. The molecular biology of matrix metalloproteinases and tissue inhibitors of metalloproteinases in inflammatory bowel diseases. *Crit Rev Biochem Mol Biol*. 2016;51:295-358.
16. López de Andrés J, Griñán-Lisón C, Jiménez G, Marchal J. Cancer stem cell secretome in the tumor microenvironment: a key point for an effective personalized cancer treatment. *J Hematol Oncol*. 2020;13:136.
17. Huang T, Song X, Xu D, et al. Stem cell programs in cancer initiation, progression, and therapy resistance. *Theranostics*. 2020;10:8721-8743.
18. Gattazzo F, Urciuolo A, Bonaldo P. Extracellular matrix: a dynamic microenvironment for stem cell niche. *Biochim Biophy Acta (BBA)-General Subjects*. 2014;1840(8):2506-2519.

19. Hanahan D, Coussens L. Accessories to the crime: functions of cells recruited to the tumor microenvironment. *Cancer Cell*. 2012;21:309-322.
20. Henke E, Nandigama R, Ergün S. Extracellular matrix in the tumor microenvironment and its impact on cancer therapy. *Front Mol Biosci*. 2020;6:160.
21. Eble J, Niland S. The extracellular matrix in tumor progression and metastasis. *Clin Exp Metastasis*. 2019;36:171-198.
22. Walker C, Mojares E, del Río Hernández A. Role of extracellular matrix in development and cancer progression. *Int J Mol Sci*. 2018;19(10):3028.
23. Kaps L, Schuppan D. Targeting cancer associated fibroblasts in liver fibrosis and liver cancer using nanocarriers. *Cells*. 2020;9(9):2027.
24. Qiu Z, Tu L, Hu X, et al. A Preliminary Study of miR-144 Inhibiting the Stemness of Colon Cancer Stem Cells by Targeting Krüppel-Like Factor 4. *J Biomed Nanotechnol*. 2020;16:1102-1109.
25. Zhang C, Zhao Y, Yang Y, et al. RNAi mediated silencing of Nanog expression suppresses the growth of human colorectal cancer stem cells. *Biochem Biophys Res Commun*. 2021;534:254-260.
26. Tang Q, Chen J, Di Z, et al. TM4SF1 promotes EMT and cancer stemness via the Wnt/β-catenin/SOX2 pathway in colorectal cancer. *J Exp Clin Cancer Res*. 2020;39:232.
27. Flores-Hernández E, Velázquez D, Castañeda-Patlán M, et al. Canonical and non-canonical Wnt signaling are simultaneously activated by Wnts in colon cancer cells. *Cell Signal*. 2020;72:109636.
28. Adam R, van Neerven S, Pleguezuelos-Manzano C, et al. Intestinal region-specific Wnt signalling profiles reveal interrelation between cell identity and oncogenic pathway activity in cancer development. *Cancer Cell Int*. 2020;20:578.
29. Clevers H, Loh K, Nusse R. Stem cell signaling. An integral program for tissue renewal and regeneration: Wnt signaling and stem cell control. *Science (New York, N. Y.)*. 2014:346:1248012.
30. Basu M, Roy S. Wnt/β-catenin pathway is regulated by PITX2 homeodomain protein and thus contributes to the proliferation of human ovarian adenocarcinoma cell, SKOV-3. *J Biol Chem*. 2013;288:4355-4367.
31. Huang C, Ma R, Xu Y, et al. Wnt2 promotes non-small cell lung cancer progression by activating WNT/β-catenin pathway. *Am J Cancer Res*. 2015;5:1032-1046.
32. Jiang H, Li Q, He C, et al. Activation of the Wnt pathway through Wnt2 promotes metastasis in pancreatic cancer. *Am J Cancer Res*. 2014;4:537-544.
33. Cancer Genome Atlas Network. Comprehensive molecular characterization of human colon and rectal cancer. *Nature*. 2012;487:330-337.

SUPPORTING INFORMATION

Additional supporting information may be found online in the Supporting Information section.

How to cite this article: Wang B, Wang X, Tseng Y, et al. Distinguishing colorectal adenoma from hyperplastic polyp by WNT2 expression. *J Clin Lab Anal*. 2021;35:e23961. https://doi.org/10.1002/jcla.23961